Supporting Informaiton

Free-Standing 3D Alkalized $Ti_3C_2T_x$/$Ti_3C_2T_x$ Nanosheet Membrane Electrode for Highly Efficient and Stable Desalination in Hybrid Capacitive Deionization

Xiaojie Shen[1, 4], Reti Hai[1], Xiaohui Wang[1], Yuan Li[1], Yayi Wang[3], Fei Yu[2*], Jie Ma[3,4,5*]*

1 Department of Environmental Science & Engineering, College of Chemical Engineering, Beijing University of Chemical Technology, 15 North Third Ring Road, Beijing 100029, P. R. China

2 College of Marine Ecology and Environment, Shanghai Ocean University, Shanghai 201306, P.R. China, E-mail: fyu@vip.163.com

3 State Key Laboratory of Pollution Control and Resource Reuse, College of Environmental Science and Engineering, Tongji University, Shanghai, 200092, P. R. China.

4 Research Center for Environmental Functional Materials, College of Environmental Science and Engineering, Tongji University, 1239 Siping Road, Shanghai 200092, P.R. China

5 Shanghai Institute of Pollution Control and Ecological Security, Shanghai, 200092, P.R. China

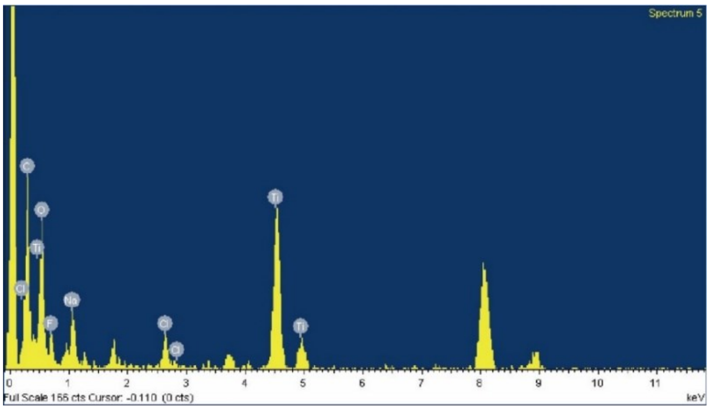

Element	Atomic %
C	52.00
O	27.03
F	3.75
Na	4.50
Cl	1.82
Ti	10.90

Figure S1. EDS elemental analysis of the Alk-$Ti_3C_2T_x$-M.

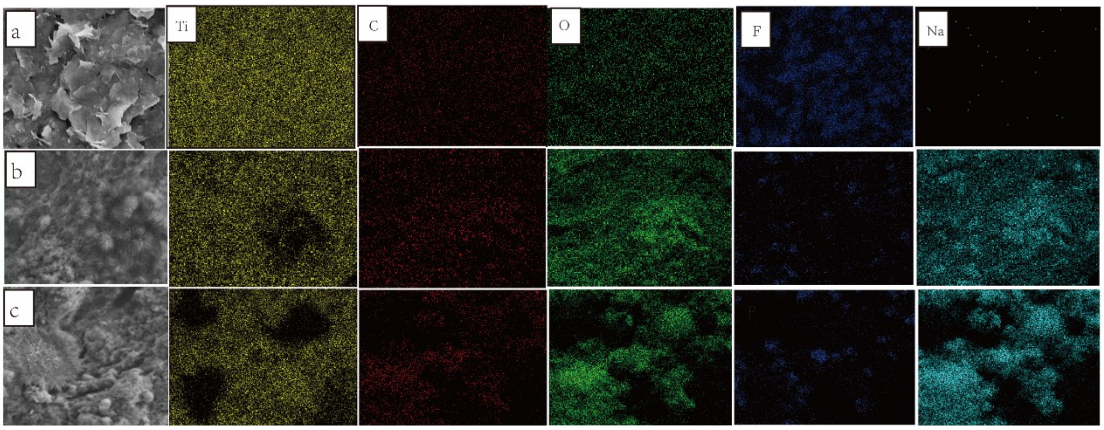

Figure S2. The elemental mapping of (a) $Ti_3C_2T_x$, (b)Alk-$Ti_3C_2T_x$ and (c)Alk-$Ti_3C_2T_x$-M.

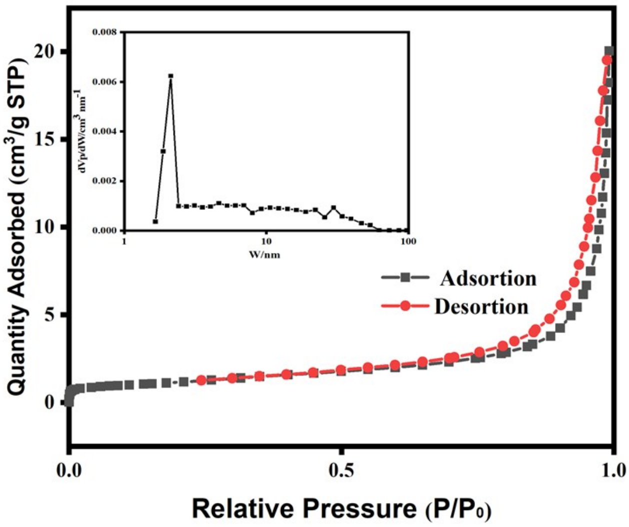

Figure S3. N_2 adsorption-desorption isotherms and the pore size distribution of d-$Ti_3C_2T_x$.

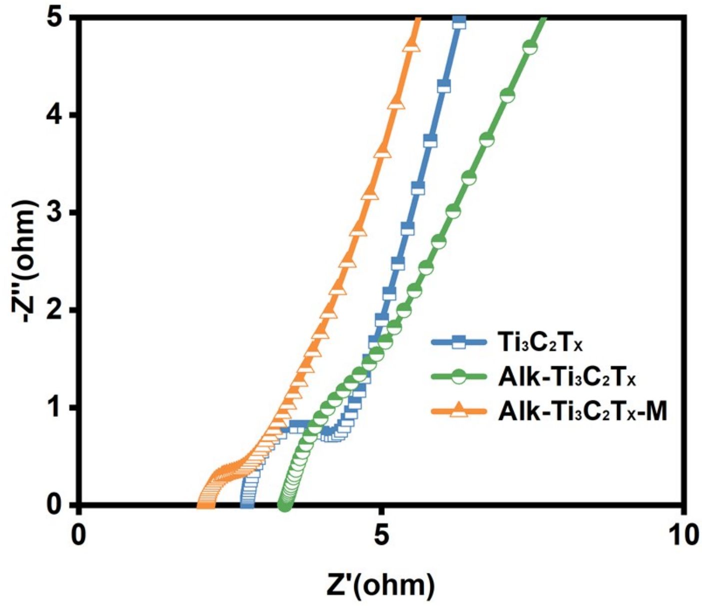

Figure S4. Nyquist plots for the $Ti_3C_2T_x$, Alk-$Ti_3C_2T_x$, and Alk-$Ti_3C_2T_x$-M electrodes.

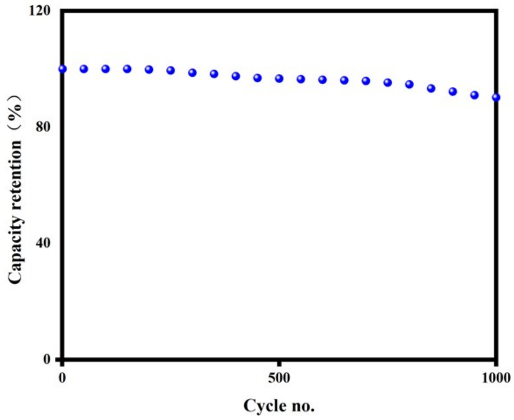

Figure S5. Cycling stability of Alk-$Ti_3C_2T_x$-M.

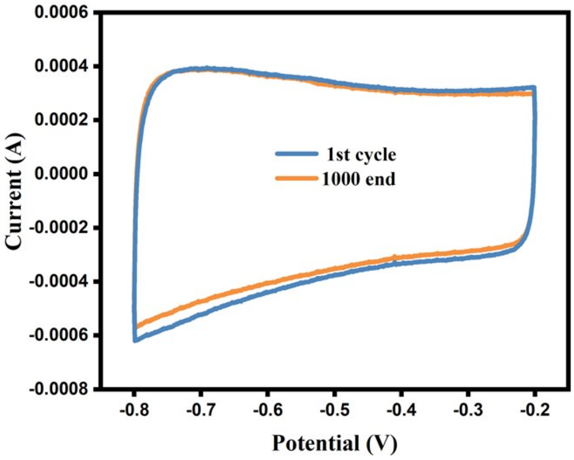

Figure S6. CV curves collected for Alk-$Ti_3C_2T_x$ -M electrodes at a scan rate of 10 mV/s before and after 1000 cycles.

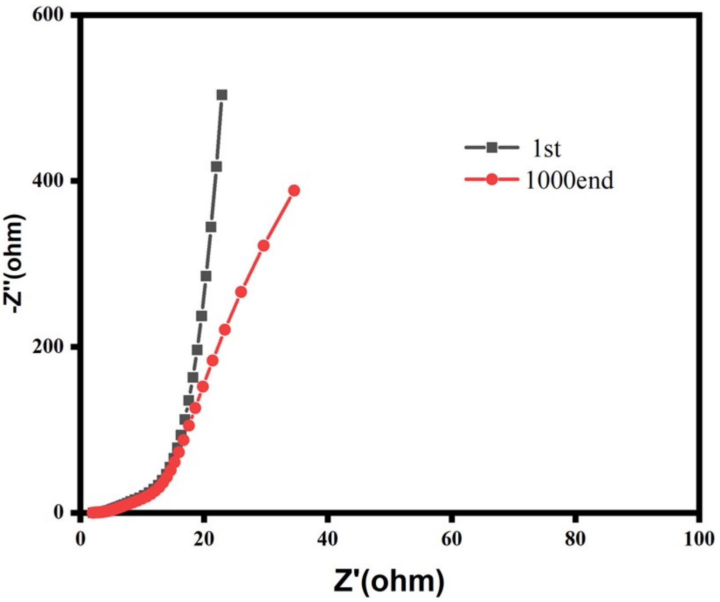

Figure S7. Nyquist plots for Alk-$Ti_3C_2T_x$-M electrodes before and after 1000 cycles.

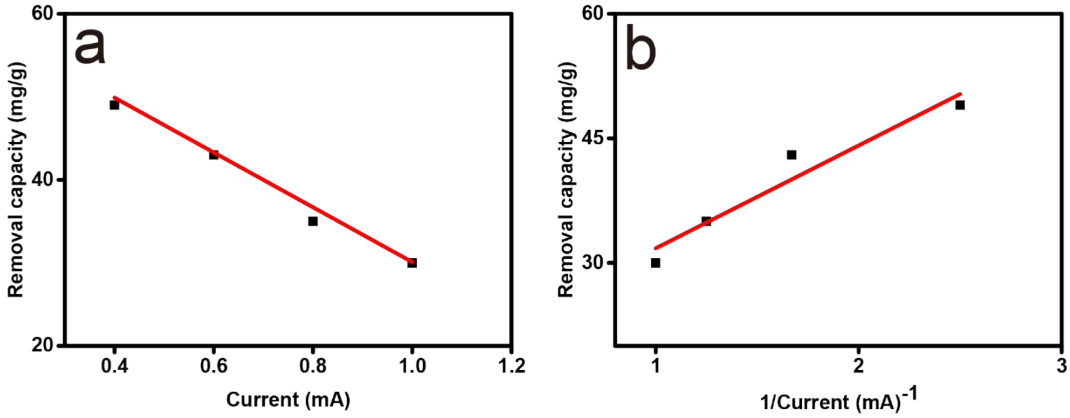

Figure S8. (a) the relationship of desalination capacity versus inverse current, (b) the relationship of desalination capacity versus the current for Alk-$Ti_3C_2T_x$-M.

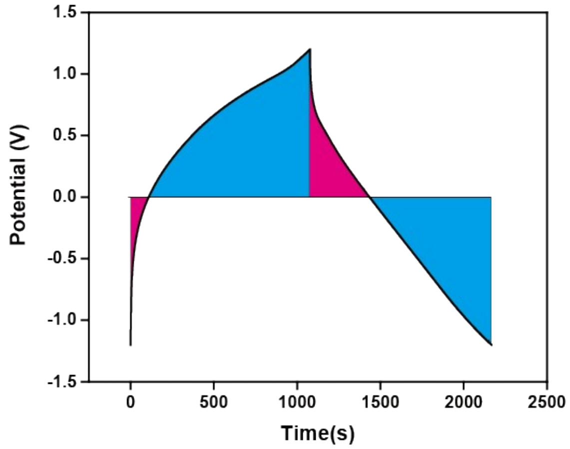

Figure S9. The energy recovery of between Alk-$Ti_3C_2T_x$-M.

In step red, the current and voltage are opposite, so the power (P=U×I) is negative which corresponds the generation of electrical energy. While in step blue, the current and voltage are in the same direction, the power is positive which corresponds the consumption of electrical energy.

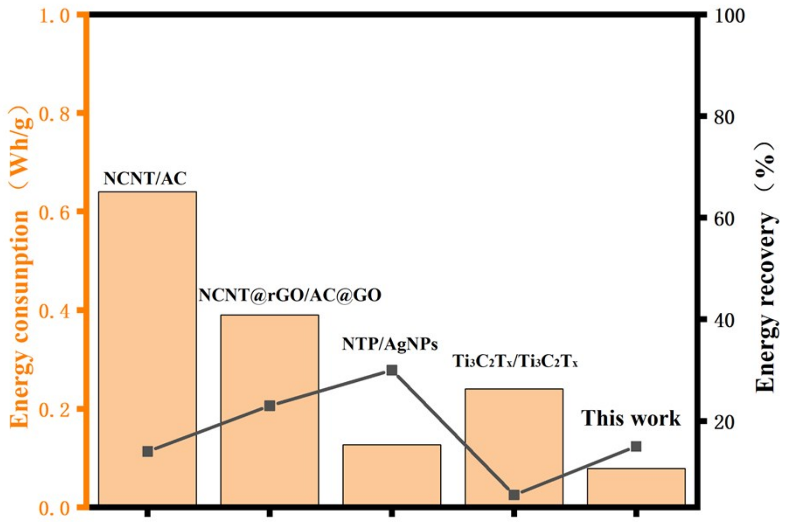

Figure S10. The energy consumption and energy recovery of between Alk-$Ti_3C_2T_x$-M and other emerging materials[1-3]

As shown in the Fig S10, compared with the NCNT/AC material based on HCDI, NTP/AgNPs based on BDI and $Ti_3C_2T_X$-CDI, the material in this study is based on HCDI (15.3%), which shows that it has lower energy consumption, and it is equivalent to HCDI (14% and 23%) in terms of energy recovery, much higher than CDI (5.44%), but a little lower than BDI (30%). It is a promising electrode material.

Table S1. XPS data of each material (Normalized EDX, at %).

Sample	C (1s)	Ti (2p)	O (1s)	F (1s)	Na (1s)
$Ti_3C_2T_x$	39.79	23.35	20.73	16.13	-
Alk-$Ti_3C_2T_x$	36.67	22.79	30.94	7.69	1.91

Table S2. Summarized C_t, C_o and C_i

Sample	C_t	C_o	C_i	C_i/ C_t
$Ti_3C_2T_x$	84.89	52.46	32.43	0.38
Alk-$Ti_3C_2T_x$	128.21	62.79	65.42	0.52
Alk-$Ti_3C_2T_x$-M	141	97.87	43.13	0.31

Table S3. Comparison of various reported electrodes applied for CDI.

Electrode materials (Cathode)	**C_0（mg /L）**	**Applied voltage/current density**	**SAC (mg/g)**	**Long term-stabillity**	**Ref.**
Ti_3C_2–MXene	292	1.2	13±2	30	[4]
porous $Ti_3C_2T_x$ MXene aerogel	10000	1.2	45	60	[5]
Ar plasma modification of 2D MXene $Ti_3C_2T_x$	500	1.4	26.8	-	[6]
$Mo_{1.33}CT_x$/CNT	35100	0.8	15	40	[7]
CNT/$NaMnO_2$	20000	1.2	42.6	100	[8]
MoS_2–10CNT-4h	150000	0.8	25	25	[9]
$Na_4Mn_9O_{18}$	15000	1.2	31.2	-	[10]
Alk-$Ti_3C_2T_x$-M	1000	30mA/g/1.2V	50	250	This work

Table S4. Comparison of the desalination capacities and rates performance among various carbon, pseudo-capacitive, and faradic electrode materials reported in the literature.

Electrodes Material	**Cell Architecture**	**Power Mode**	**Voltage/Current**	**C_o (mg/L)**	**SAC（mg/g）**	**ADR (mg/g/s)**	**Ref**
Porous Carbon	CDI	C.V.	1.2 V	50	2.2	0.0360	[11]
		C.V.	1.2 V	50	6.6	0.0160	
Activate Carbon	MCDI	C.C.	1.2V/2.0 mA	584.4	4.2	0.0830	[12]
		C.C.	1.2V/5.0 mA	584.4	6.8	0.0890	
		C.C.	1.2V/9.0 mA	584.4	10.0	0.0745	
		C.C.	1.2V/15.0 mA	584.4	15.7	0.0410	
$Na_2FeP_2O_7$	HCDI	C.C.	1.2V/3.0 mA/cm^2	584.4	7.8	0.0680	[13]
		C.C.	1.2V/2.0 mA/cm^2	584.4	12.8	0.0450	
		C.C.	1.2V/1.5m A/cm^2	584.4	16.9	0.0340	
		C.C.	1.2V/1.0 mA/cm^2	584.4	24.0	00220	
Nafion-coated AC	RCDI	C.C.	1.2 V/1.0 mA/cm^2	1168.8	19.10	0.0378	[14]
		C.C.	1.2 V/1.0 mA/cm^2	1168.8	25.9	0.0313	
		C.C.	1.2 V/1.0 mA/cm^2	1168.8	30.40	0.0270	
		C.C.	1.2 V/1.0 mA/cm^2	1168.8	35.60	0.0216	
BiOCl| Na0.44MnO2	Dual-ion electrochemical desalination	C.C.	1.5 V/100 mA/g	760.0	68.5	0.021	[15]
		C.C.	1.5 V/200 mA/g	760.0	37.5	0.041	
		C.C.	1.5 V/300 mA/g	760.0	22.4	0.062	
		C.C.	1.5 V/500 mA/g	760.0	9.2	0.092	
Alk-$Ti_3C_2T_x$-M	HCDI	C.C.	1.2V/100 mA/g	1000	31	0.052	This work
		C.C.	1.2V/80 mA/g	1000	37	0.045	
		C.C.	1.2V/60 mA/g	1000	45	0.038	
		C.C.	1.2V/40 mA/g	1000	53	0.030	

Table S5. Energy consumption of different desalination methods with different electrode materials.

Materials	**Cell Architecture**	**Energy consumption （kWh/Kg）**	**Ref.**
RO	RO	0.47	[16]
Activated carbon	CDI	1.11	[17]
Membrane assisted CDI	MCDI	0.64	[18]
NVP@C	HCDI	0.46	[19]
$NaTi_2(PO_4)_3$-AgNPs electrodes	BDI	0.127	[2]
Alk-$Ti_3C_2T_x$-M	HCDI	0.079±0.02	This work

References

1. D. Sriramulu and H. Y. Yang, *Nanoscale*, 2019, **11**, 5896-5908.
2. Y. X. Huang, F. M. Chen, L. Guo, J. Zhang, T. P. Chen and H. Y. Yang, *Desalination*, 2019, **451**, 241-247.
3. J. Ma, Y. J. Cheng, L. Wang, X. H. Dai and F. Yu, *Chem. Eng. J.*, 2020, **384**, 8.
4. P. Srimuk, F. Kaasik, B. Kruner, A. Tolosa, S. Fleischmann, N. Jackel, M. C. Tekeli, M. Aslan, M. E. Suss and V. Presser, *J. Mater. Chem.*, 2016, **4**, 18265-18271.
5. W. Z. Bao, X. Tang, X. Guo, S. Choi, C. Y. Wang, Y. Gogotsi and G. X. Wang, *Joule*, 2018, **2**, 778-787.
6. L. Guo, X. F. Wang, Z. Y. Leong, R. W. Mo, L. Sun and H. Y. Yang, *Flatchem*, 2018, **8**, 17-24.
7. P. Srimuk, J. Halim, J. Lee, Q. Z. Tao, J. Rosen and V. Presser, *ACS Sustainable Chem. Eng*, 2018, **6**, 3739-3747.
8. S. Y. Wang, G. Wang, X. P. Che, S. F. Wang, C. X. Li, D. Z. Li, Y. Q. Zhang, Q. Dong and J. S. Qiu, *Environ. Sci.: Nano*, 2019, **6**, 2379-2388.
9. P. Srimuk, J. Lee, S. Fleischmann, S. Choudhury, N. Jackel, M. Zeiger, C. Kim, M. Aslan and V. Presser, *J. Mater. Chem. A,*, 2017, **5**, 15640-15649.
10. J. Lee, S. Kim, C. Kim and J. Yoon, *Energy Environ. Sci*, 2014, **7**, 3683-3689.
11. M. Wang, X. T. Xu, Y. Liu, Y. J. Li, T. Lu and L. K. Pan, *Carbon*, 2016, **108**, 433-439.
12. T. Kim and J. Yoon, *Rsc Adv*, 2015, **5**, 1456-1461.
13. S. Kim, J. Lee, C. Kim and J. Yoon, *Electrochim. Acta*, 2016, **203**, 265-271.
14. J. Lee, K. Jo, J. Lee, S. P. Hong, S. Kim and J. Yoon, *ACS Sustainable Chem. Eng*, 2018, **6**, 10815-10822.
15. F. M. Chen, Y. X. Huang, L. Guo, L. F. Sun, Y. Wang and H. Y. Yang, *Energy Environ. Sci*, 2017, **10**, 2081-2089.
16. R. Zhao, S. Porada, P. M. Biesheuvel and A. Van der Wal, *Desalination*, 2013, **330**, 35-41.
17. C. Kim, P. Srimuk, J. Lee, M. Aslan and V. Presser, *Desalination*, 2018, **425**, 104-110.
18. H. Yoon, J. Lee, S. Kim and J. Yoon, *Desalination*, 2017, **422**, 42-48.
19. J. L. Cao, Y. Wang, L. Wang, F. Yu and J. Ma, *Nano Lett.*, 2019, **19**, 823-828.